Desalination and Water Treatment
www.deswater.com
doi: 10.5004/dwt.2020.26297

206 (2020) 189–201
December

Pretreatment process optimization and reverse osmosis performances of a brackish surface water demineralization plant, Morocco

Hicham Boulahfa[a,*], Sakina Belhamidi[a], Fatima Elhannouni[a], Mohamed Taky[a], Mahmoud Hafsi[b], Azzedine Elmidaoui[a]

[a]*Laboratory of Separation Processes, Department of Chemistry, Faculty of Sciences, Ibn Tofail University, P.O. Box: 1246, Kenitra 14000, Morocco, emails: boulahfa.hi@gmail.com (H. Boulahfa), sakina.belhamidi@uit.ac.ma (S. Belhamidi), fatima.elhannouni@uit.ac.ma (F. Elhannouni), mohamed.taky@uit.ac.ma (M. Taky), azzedine.elmidaoui@uit.ac.ma (A. Elmidaoui)*
[b]*International Institute for Water and Sanitation, National Office of Electricity and Potable water (ONEE-IEA), Rabat, Morocco, email: mahmoud.hafsi@onee.ma (M. Hafsi)*

Received 6 January 2020; Accepted 29 June 2020

ABSTRACT

In surface water reverse osmosis (RO) demineralization processes, pretreatment is a key step in achieving high performances and avoiding frequent membrane fouling. The plant studied includes conventional pretreatment and RO process. The aim of this study is the optimization of the coagulation–flocculation and the assessment of its effect on pretreated water quality upstream of the RO unit. The monitored parameters were turbidity, residual aluminum, and silt density index (SDI). Moreover, this paper presents the RO membrane performance in terms of feed pressure, pressure drop, permeate flow, and permeate conductivity after nearly 1 y of operation. The results obtained illustrate that the pretreatment optimization substantially reduces the residual aluminum concentration and the SDI after the 5 μm cartridge filters. Likewise, the RO membranes exhibited high and steady performance.

Keywords: Surface water; Pretreatment; Reverse osmosis; Fouling; Demineralization

1. Introduction

Over the last years, water shortage becomes one of the great challenges in many locations around the world [1–4]. Thus, in order to meet the increasing demand for fresh water, desalination of seawater, and brackish water were performed using reverse osmosis (RO) membrane technology to provide drinking water [5–9]. Nonetheless, RO is currently the most energy-efficient technology for desalination, with the energy consumption ranges between 1.5 and 2.5 kWh/m^3, which is much lower than that of other technologies [10,11]. Furthermore, energy consumption depends on the plant operating conditions [12,13].

However, RO membrane performance is significantly affected by the membrane fouling [14–17]. In fact, passing the raw water directly via the RO membranes can cause irreversible fouling [18]. Hence, in order to control membrane fouling, a variety of processes such as pretreatment, membrane monitoring, membrane chemical cleaning, surface modification, as well as developing novel RO membranes have been studied [19–23].

RO systems had widely carried out pretreatment technologies. These technologies had the advantage of enhancing the feed water quality mainly to ensure reliable RO exploitation as well as to prolong membrane life [24]. Among all the processes, conventional water treatment methods include coagulation, flocculation, and sedimentation processes, usually followed by filtration and disinfection [25].

* Corresponding author.

Coagulation–flocculation is considered the most crucial method in surface water treatment, and it can be used as a pretreatment, post-treatment, or even main treatment [25,26]. Some parameters may affect the aggregation of colloids, pH, turbidity, chemical composition of the raw water samples, coagulant dosage, water temperature, surface area of colloids, and mixing conditions [27–30]. Coagulation is the process of destabilizing suspended solids. Coagulants and colloids possess adverse electrical charges in water and thus when they meet the charges could be neutralized, resulting in fast aggregation of small suspended particles to form microflocs [31–33].

In addition, coagulants are extensively used in the treatment of public water supply systems [25,34]. Among all the coagulants, Al-based coagulants have been used most widely, and they can change surface charge properties to promote agglomeration and/or enmeshment of smaller particles into larger flocs [27–29,35,36]. However, it raised more concerns due to the increase of residual aluminum in treated water, which can cause even more issues [29,35,37].

Researchers have studied the effects of solution pH, coagulant dosage, characteristics of coagulants, and water temperature on residual aluminum [36,37].

The Khenifra RO desalination plant was the first water treatment plant in Morocco, which combined conventional treatment with RO process. The plant will cover the production of 36,290 m^3/d of potable water by the year 2030 [30].

The present work aimed to optimize the coagulation–flocculation processes as pretreatment for the RO membranes. The coagulation–flocculation was performed using aluminum sulfate, polyelectrolyte, and settled sludge recirculation at the flocculation level. The different parameters ware studied at various pH values in order to optimize residual aluminum inlet of RO membranes. Therefore, the pretreatment process performance was assessed after the application of the chemical dosages defined previously at the laboratory scale by jar-tests. However, the performance of the RO membranes was evaluated in terms of feed pressure, pressure drop, permeate flow, and permeate conductivity.

2. Materials and methods

2.1. Feed water characteristics

The surface water was provided from the Tanfnit dam located at about 15 km of the desalination plant. The feed water experienced significant seasonal variations in terms of turbidity, temperature, and conductivity [30,38].

Table 1 presents the main characteristics of the raw water.

2.2. Coagulation–flocculation jar test

In order to study the effects of the coagulant dosage, the polymer dosage, the settled sludge recirculation, and the pH variation on the residual aluminum and the turbidity removal. Jar tests were performed on a six-paddle gang stirrer (VELP – JTL6), including rapid mixing (120 rpm for 2 min) after addition of aluminum sulfate followed by slow mixing (40 rpm for 20 min), after which the suspension was settled for 30 min. After sedimentation, the samples were withdrawn and measured to determine residual aluminum [36]. The pH values of water samples were adjusted by sulfuric acid H_2SO_4 solution 98%.

Table 1
Raw water characteristics used for the RO system design

Parameter	Average value
pH	8.02
Alkalinity TAC, °F	17.6
Calcium (mg/L)	95
Magnesium (mg/L)	32.5
Sodium (mg/L)	466
Potassium (mg/L)	2.9
Manganese (mg/L)	0
Ammonium (mg/L)	0
Iron (mg/L)	<0.03
Baryum (mg/L)	0
Bicarbonate (mg/L)	214
Chloride (mg/L)	866
Sulfate (mg/L)	117
Nitrate (mg/L)	6.49
Fluoride (mg/L)	0
Total dissolved solids (TDS) (mg/L)	1,800

The optimization of the sodium bisulfate was carried out using stoichiometric calculations. The obtained dose to neutralize 1 mg/L of free chlorine was 1.34 mg/L of sodium bisulfate [30].

The antiscalant Genesys LF dose was performed using Genesys MM4 software version V1.22.1 (DLL.V1.8.7) [38]. The obtained dose was 2.4 mg/L with pH adjustment and 3 mg/L without pH adjustment [30].

2.3. Process description

Khenifra plant process includes conventional treatment, acidification (H_2SO_4) to reduce the precipitation of calcium carbonate ($CaCO_3$) at the membrane level, injection of the antiscalants to reduce the precipitation of calcium sulfate ($CaSO_4$) at the membrane surface, microfiltration using 5 μm cartridge filters, and dechlorination using sodium bisulfate [30,39].

This brackish water RO desalination plant was designed to produce 36,290 m^3/d of drinking water at the horizon of the year 2030 [30]. The RO system (Fig. 1) includes three trains, each train with one pass and two stages. The first stage and the second stage contain 52 and 23 pressure vessels, respectively. Each pressure vessel was loaded with seven FilmTec™ XLE440 RO elements made in USA [30,38].

The RO membranes installed were 8″ spiral wound membrane elements (FILMTEC™ XLE440, USA). From the manufacturer, the permeate flow and salt rejection of the membrane elements under the standard conditions were 36.8 L/min and 99.5%, respectively (standard conditions: 2,000 ppm NaCl, 125 psi (8.6 Bar), 77°F (25°C), pH 8, and 15% recovery) [30].

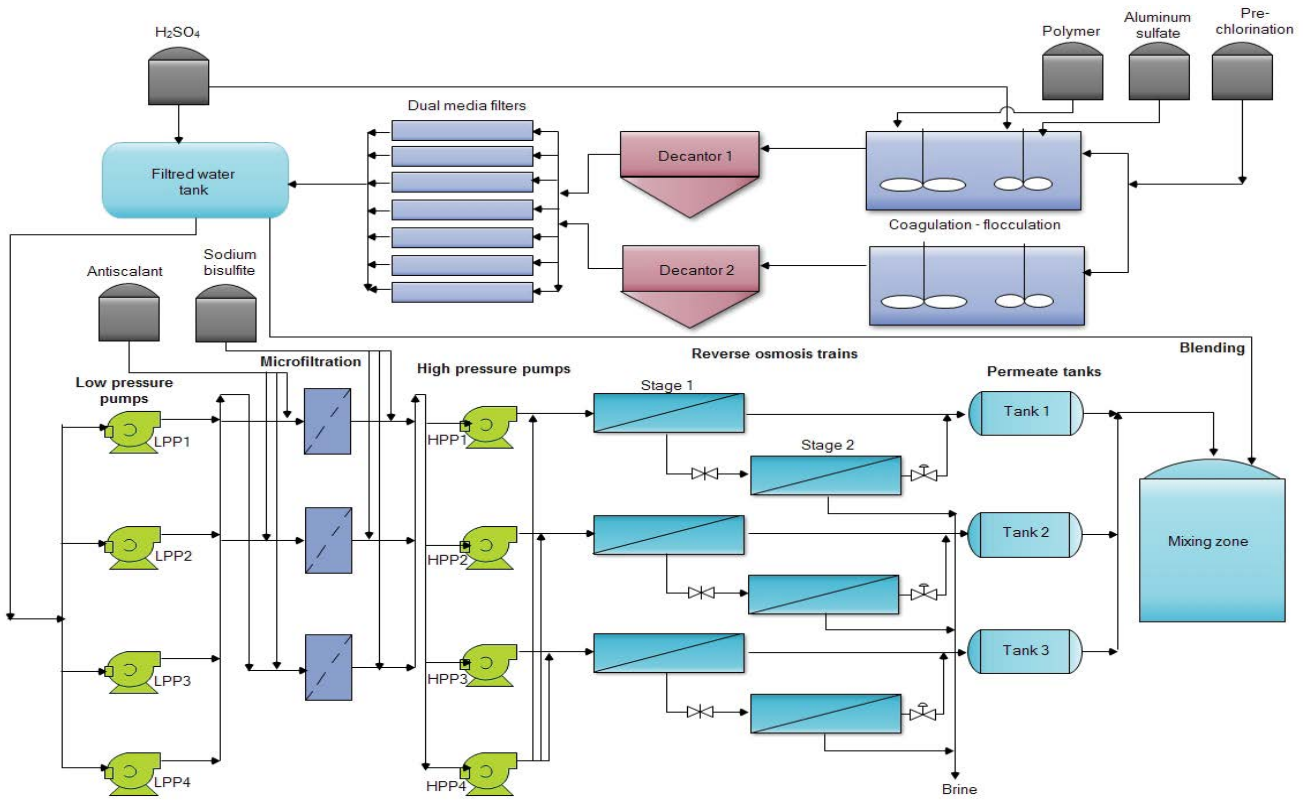

Fig. 1. Flow chart of the Khenifra desalination plant [38].

3. Results and discussion

3.1. Pretreatment optimization

To illustrate the chemicals injection effect on treated water quality, multiple tests were carried out based on the actual surface water quality. The raw water characteristics are listed in Table 2.

3.1.1. Effect of the coagulant injection on the pretreatment performance

Fig. 2 shows the evolution of the turbidity and the residual Al as a function of the aluminum sulfate injected dose. Fig. 2 illustrates that the optimal dosage of the aluminum sulfate was 20 mg/L. Indeed, this dosage corresponds to the turbidity and the residual aluminum concentration of 0.35 NTU and 0.14 mg/L, respectively.

With regard to the coagulant effect, determining the "right" quantity is a prerequisite for optimized efficiency. Thus, an overdose of the coagulant results in a substantial increase in the amount of sludge and a decrease in pH, while a lower dose is usually the cause of the residual metals remaining in the treated water [27,35,40–41]. Hence, the need to strengthen the coagulation processes [42,43].

The turbidity and the residual aluminum values obtained in this test did not meet the pretreatment requirements and the Moroccan standard. Hence, the need to perform another testing to achieve the pretreatment objectives.

Table 2
Characteristics of the raw water samples

Parameter	Value
pH	8.02
Turbidity, NTU	45.6
Oxydability, mg/L	2.8
TAC, °F	25
Iron, mg/L	0
Manganese, mg/L	0

3.1.2. Effect of the polymer injection on the pretreatment performance

The polymers are generally natural compounds or macromolecular synthetic of chemical units repetitive (monomers) and are capable of destabilizing the constituents of an aqueous environment, thus improving their flocculation [41].

To explain the polymer injection effect on the raw water treatment, the coagulant dosage determined previously was applied and the polymer dosage was varied.

Fig. 3 describes the polymer injection effect on the pretreated water turbidity and residual aluminum. As can be seen in Fig. 3, at a constant aluminum sulfate dosage of 20 mg/L and a constant pH, the best dosage of the anionic

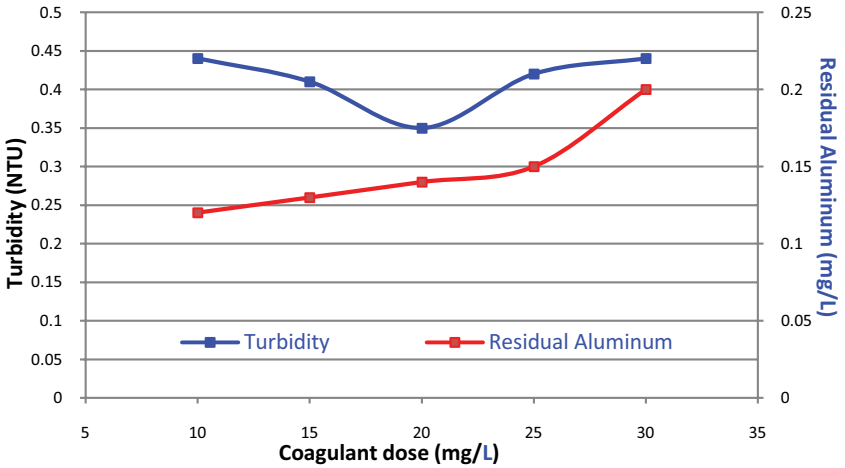

Fig. 2. Effect of various coagulant dosages on turbidity removal and residual Al.

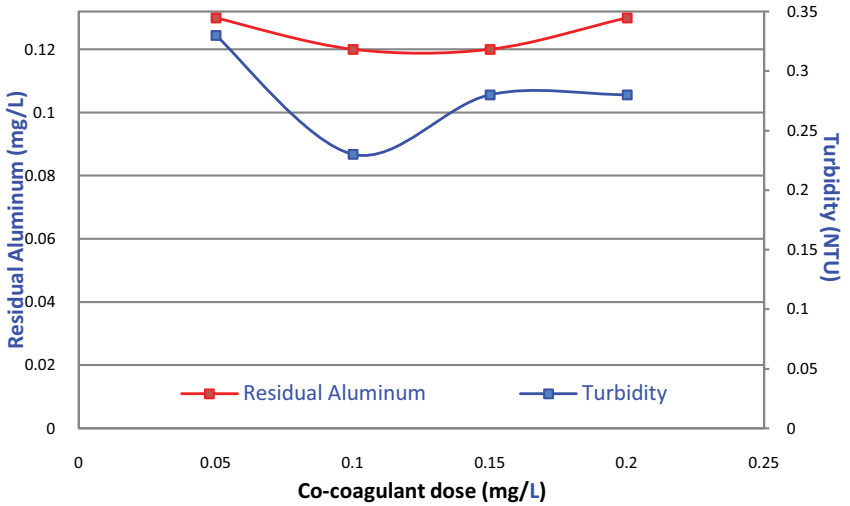

Fig. 3. Effect of the polymer dosages on turbidity removal and residual aluminum.

polymer was 0.10 mg/L, which corresponds to turbidity of 0.23 NTU and a residual aluminum concentration of 0.12 mg/L. In fact, the polymer allows the adhesion of micro flocs formed during the coagulation process, the formation of large flocs, and therefore the flocculation improvement [44].

The polymer injection with the coagulant optimal dosage significantly reduced the turbidity value and slightly the residual aluminum concentration compared to the treatment with only the aluminum sulfate injection.

3.1.3. Effect of the pH variation on the pretreatment performance

To highlight the acidification influence upstream of the coagulation–flocculation on the filtered water quality, in terms of turbidity and residual aluminum. Jar-tests were performed by applying the aluminum sulfate and polymer doses defined previously with the pH variation.

Fig. 4 shows the pH variation effect on the turbidity and the residual Al concentration at constant dosages of aluminum sulfate and polymer.

The results obtained demonstrate that the pH variation has a significant effect on the residual Al reduction [36,37]. Indeed, at pH 6.5, the residual Al value was 0.07 mg/L, a decrease of approximately 42% compared to the aluminum sulfate, and polymer injection without pH adjustment (turbidity has also decreased to 0.2 NTU). In effect, the pH variation has an influence on the training of hydroxides destabilization and as a result an effect on residual Al [29]. As the pH increased, the Al hydrolyzed according to the sequence [29]:

$$Al^{3+} \rightarrow Al(OH)^{2+} \rightarrow Al(OH)^{2+} \rightarrow Al(OH)_3 \rightarrow Al(OH)^{4-} \quad (1)$$

The most important factor that affects the coagulants efficiency to the metal base is the pH [45]. For example, when the aluminum is added to water, the hydrolysis reactions

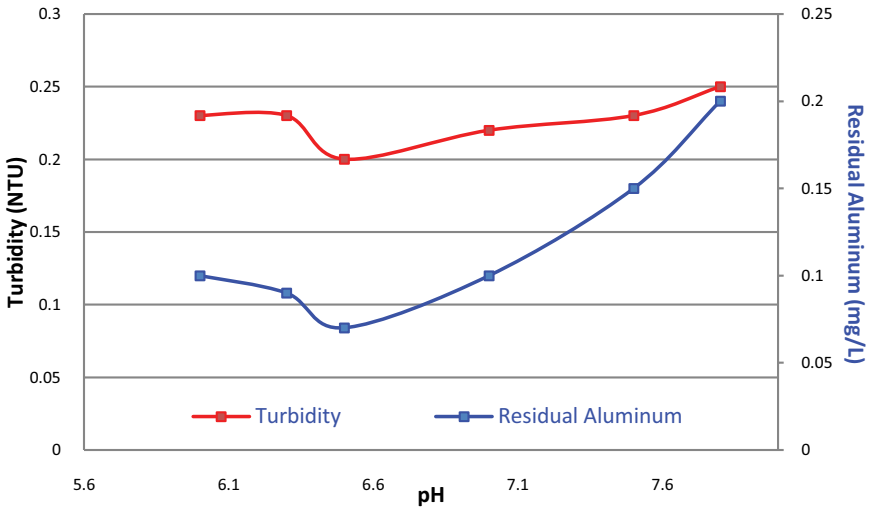

Fig. 4. Effect the pH variation on residual aluminum.

generate dissolved monomers. The species of aluminum and aluminum hydroxide precipitate and the distribution of these species depend on the pH of the minimum solubility and the total concentration of aluminum [46].

3.1.4. Effect of the settled sludge recirculation on the pretreatment performance

In order to improve the coagulation–flocculation performance, we consistently try to find the best combination that allows producing a pretreated water quality in compliance with the treatment requirements and the RO membrane manufacturer recommendations.

To achieve this goal, a jar test was conducted using settled sludge recirculation at the flocculation stage.

To determine the aluminum sulfate optimum dosage and the amount of sludge to recirculate, several jar tests were performed. The objective is to define the aluminum sulfate dosage with a constant concentration of the sludge suspended solids (SS). Once the sludge quantity is defined, further tests have been carried out to fix the aluminum sulfate optimal dosage to be applied.

3.1.4.1. Variation of the aluminum sulfate at constant sludge recirculation

In order to highlight the sludge recirculation effect on the optimization of the coagulant treatment rate, the sludge SS concentration in the flocculated water was set at 150 mg/L. The polymer dose was fixed at 0.10 mg/L and the coagulant dose was varied between 10 and 25 mg/L.

Fig. 5 illustrates the sludge recirculation effect on the filtered water turbidity and the residual Al concentration. The obtained results showed that under the test conditions, sludge recirculation reduced the filtered water turbidity of 25% and the aluminum sulfate dosage at 15 mg/L instead of 20 mg/L, is a reduction in coagulant consumption of about 25%. On the other hand, it was found that the residual aluminum concentration increased by 33% compared to the result obtained with treatment without sludge recirculation.

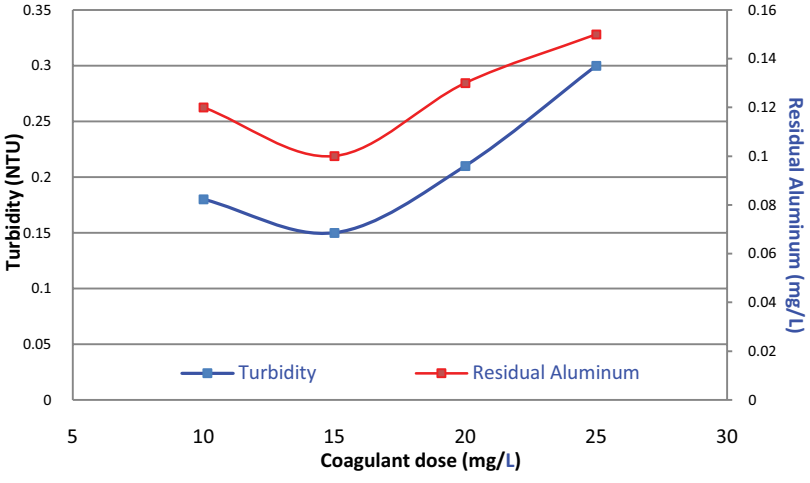

Fig. 5. Effect of sludge recirculation on turbidity removal and filtered water residual Al.

In fact, the residual Al increased significantly with the suspended solids concentration of the sludge.

3.1.4.2. Variation of the suspended solids concentration of the recirculated sludge

To illustrate the sludge recirculation effect on the coagulant and polymer doses optimization, the sludge concentration of flocculated water was varied between 100 and 250 mg/L, the polymer, and coagulant doses were set at 0.1 and 15 mg/L, respectively.

Fig. 6 indicates the sludge recirculation effect on the filtered water turbidity and residual aluminum. When the flocculated water suspended solids varied, the settled water and the filtered water turbidity were directly influenced.

Under the conditions of the test, the optimum suspended solids concentration of the recirculated sludge was 200 mg/L. Indeed, this concentration makes it possible to have filtered water turbidity of 0.12 NTU and a residual Al concentration of 0.1 mg/L. This will have a direct effect on the decanters and sand filters, which leads to a decrease of the sand filters washing frequency. Note that washing is coupled with a loss of energy and filtered water. It is therefore essential to perform this recirculation to reduce the production cost in terms of coagulant consumption, energy, and filtered water. On the other hand, it is necessary to improve the filtered water quality in terms of the residual aluminum to avoid high aluminum concentration inlet of the RO membranes.

3.1.5. Effect of the pH variation at constant suspended solids recirculation on the pretreatment performance

Fig. 7 presents the acidification effect on the filtered water quality with an injection of 15 mg/L aluminum sulfate, 0.10 mg/L polymer, and 200 mg/L sludge suspended solids.

The optimum pH for the pretreatment with sludge recirculation was 6.5. In fact, this pH value allowed reaching the turbidity of 0.12 NTU and the Al concentration of 0.07 mg/L. Therefore, acidification reduces residual aluminum by 37.5%.

The obtained results showed that the pH variation has a significant effect on the reduction of the residual Al concentration [36,37]. Indeed, the pH variation has an influence on the destabilization of the hydroxides formation and therefore an effect on the residual Al [29].

Table 3 summarizes the jar tests performed at the laboratory scale. Table 3 indicated clearly that the best combination was the test *F*. This combination leads with the best turbidity and residual aluminum.

3.2. Assessment of the pretreatment performances

The optimization carried out on the laboratory scale was applied to the pretreatment process. As shown in Fig. 8, the filtered waterturbidity showed a stable behavior, it was low all over the monitoring period. The values fluctuated between 0.09 and 0.34 NTU, recorded as maximum only once.

The turbidity fluctuations were due to the suspended solids variation at the flocculation level, clogging of sand filters, or chemical injection problems. The obtained result complies with the requirements of the guarantee, which is 0.3 NTU.

Fig. 9 exhibits the variation of the filtered water residual aluminum. The residual aluminum varied in the range of 0.05 and 0.12 mg/L. The average value recorded during the monitoring period was 0.07 mg/L.

To assess the residual Al behavior through the 5 µm cartridges. Monitoring of filtered and micro-filtered water was carried out. The results obtained in Fig. 10 illustrates that the filtered water residual aluminum decreased significantly, as it passed through the microfiltration and diminished of approximately 37%. This demonstrates that 5 µm cartridges help to reduce the residual Al concentration upstream of RO membranes.

Fig. 11 shows the water oxidability evolution through the treatment process. The average values of the raw water oxidability, filtered water, and microfiltered water were in the range of 2.51, 1.78, and 2.02 mg/L, respectively. This means a 29% decrease between raw water and filtered water and a 13% increase between filtered water and microfiltered water.

This increase was due to the addition of the phosphonate-based sequestering agent rich in organic matter and

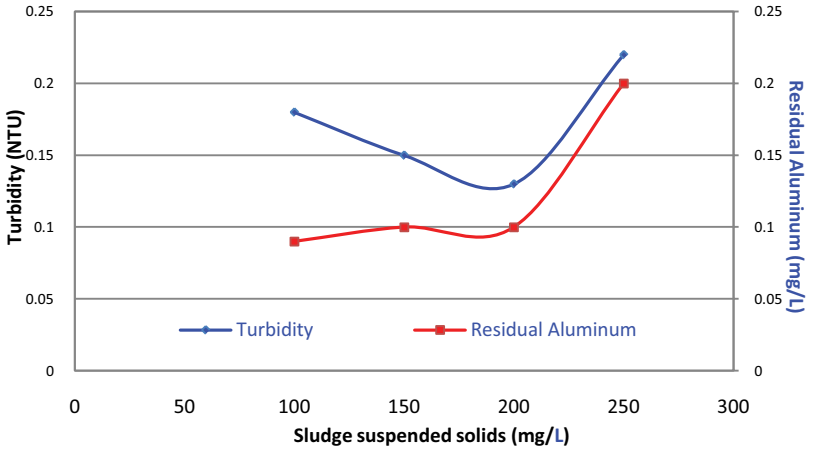

Fig. 6. Effect of the sludge recirculation on turbidity removal and residual Al.

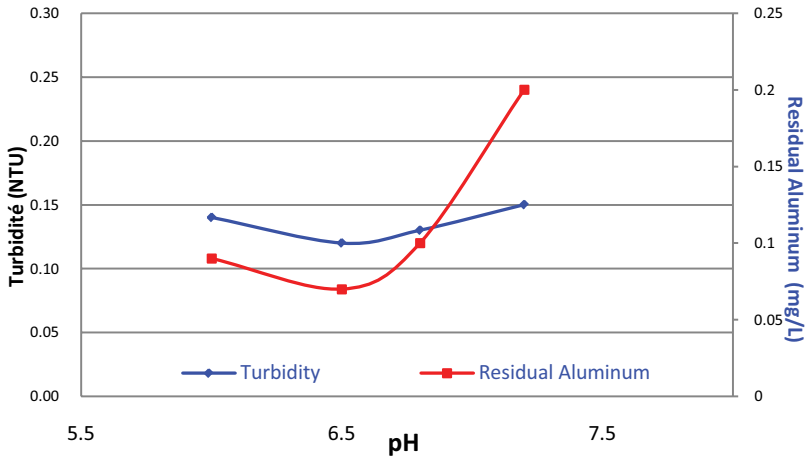

Fig. 7. Effect of the pH variation on residual Al.

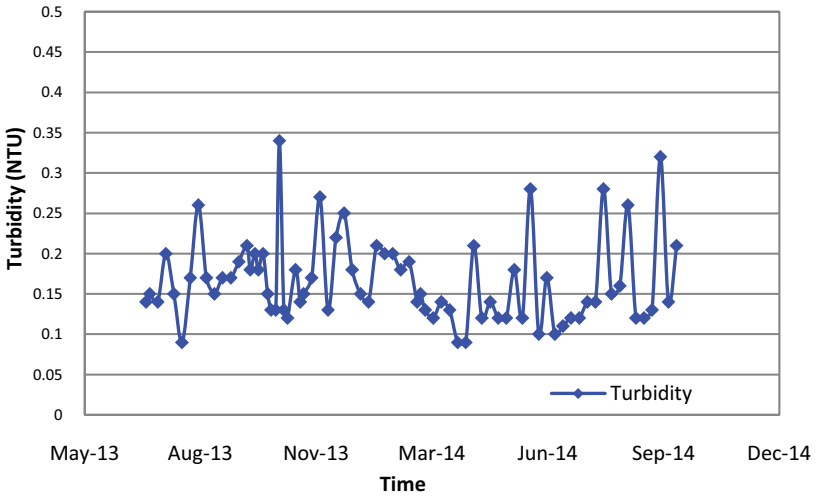

Fig. 8. Filtered water turbidity.

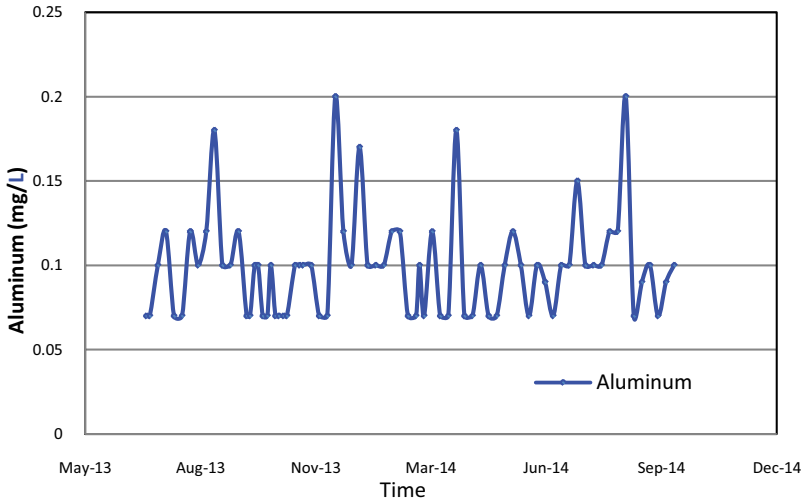

Fig. 9. Filtered water residual aluminum.

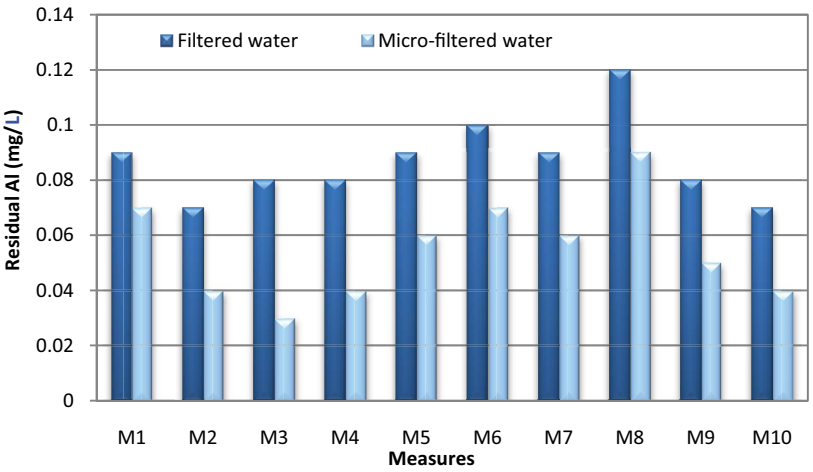

Fig. 10. Evolution of the residual Al after the microfiltration.

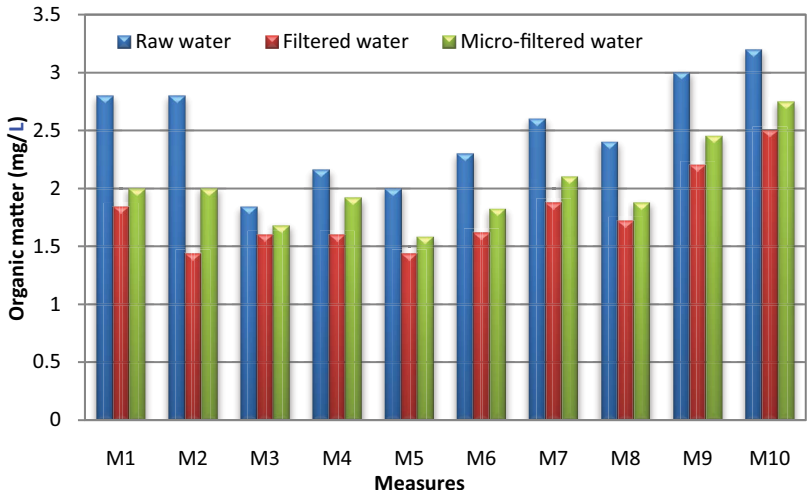

Fig. 11. Evolution of the organic matter.

Table 3
Summary of the jar tests carried out

N°	Jar tests	Coagulant dose (mg/L)	Polymer dose (mg/L)	Sludge suspended solids (g/L)	pH	Filtered water turbidity (NTU)	Residual Al (mg/L)
A	Coagulant	20	0	0	8.03	0.35	0.14
B	Coagulant + polymer	20	0.10	0	8.04	0.23	0.12
C	Coagulant + polymer + H_2SO_4	20	0.10	0	6.50	0.20	0.07
D	Coagulant + polymer + sludge	15	0.10	0.10	8.02	0.15	0.10
E	Coagulant + polymer + sludge	15	0.10	0.15	8.00	0.13	0.10
F	Coagulant + polymer + sludge + H_2SO_4	15	0.10	0.20	6.50	0.12	0.07

constitutes a source of phosphorous [47–49]. This significantly boosted oxidability values after the microfiltration.

The SDI is an indicator of the colloids and suspended particulate matter present in water [30,50–52]. Fig. 12 presents the SDI evolution of filtered water supplied from the dual media filters and micro-filtered water after the 5 μm cartridge filters; the graph shows the effectiveness of the pretreatment process; it illustrates that the SDI values were always lower than those of the design (<3) after microfiltration [30].

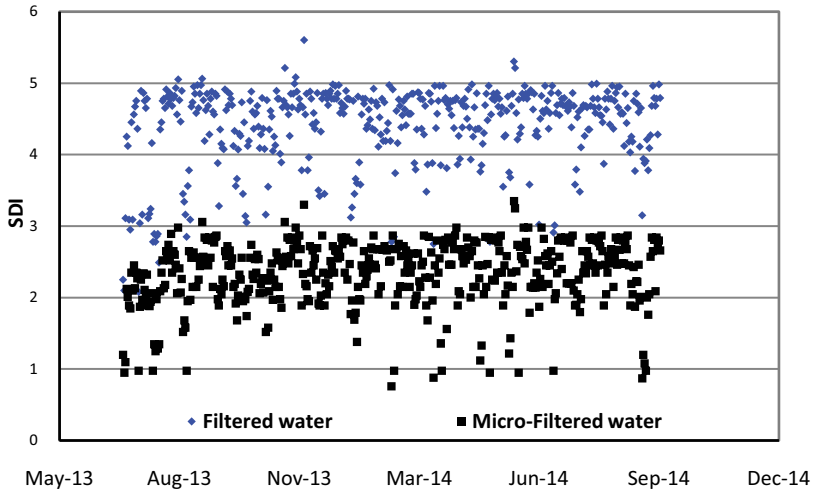

Fig. 12. Filtered and micro-filtered water SDI.

The obtained results prove that the pretreatment process inlet RO section operated successfully, and the microfiltration enhances the filtered water quality in terms of SDI [30].

4. Reverse osmosis performance assessment

Figs. 13–16 exhibit the RO unit performance, mainly the fluctuation of feed pressure, differential pressure, product flow, and permeate conductivity [38].

The plant monitoring aims to provide details that enable corrections to reduce the fouling problems or ideally to anticipate fouling. The RO unit that is the subject of this study has experienced several ups and downs from October 2013 to July 2014 [38].

From October 2013 to June 2014, the feed pressure varied substantially. It began to increase progressively and remarkably due to the augmentation of the feed water salt concentration and the temperature fluctuations [30,38]. The feed pressure augmented about 16% and 14.3% in the first and second stages, respectively, after nearly 2 months (Fig. 13). During the same period, the pressure drop was enhanced in both stages and followed up the evolution of the feed pressure (Fig. 15). The permeate flux remained stable in both stages (Fig. 14) due to the automatic regulation linked to the high-pressure pump that controlled the permeate set point regardless of the pressure increase [30,38]. The conductivity was relatively steady in the first stage and slightly increased in the second stage (Fig. 16). This can be attributed to the augmentation of the feed water salt concentration due to the surface water seasonal variation [30,38].

From December 2013 to May 2014, the feed pressure of the two stages declined gradually. After nearly 2 months of operation, the pressure stabilized around the start-up value in both stages. This immediately affected the pressure drop, although the permeate flow showed stable behavior. The permeate conductivity increased progressively in both stages. This boost is owing to the seasonal variations of the raw water salts concentration [38].

During June 2014, compared to the start-up value the feed pressure suddenly increased about 21.5% and 28.6%

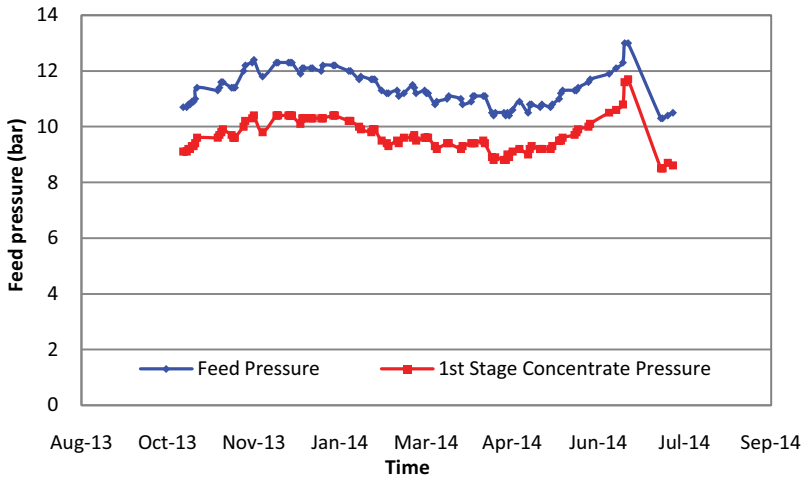

Fig. 13. Feed pressure evolution.

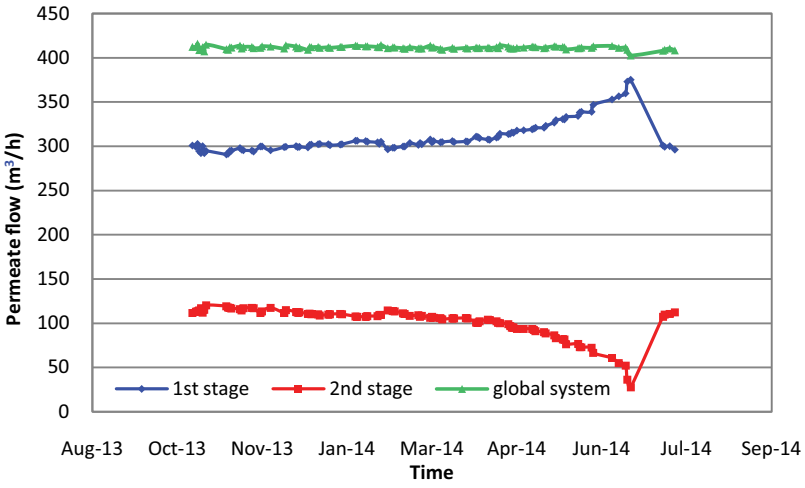

Fig. 14. Permeate flow evolution.

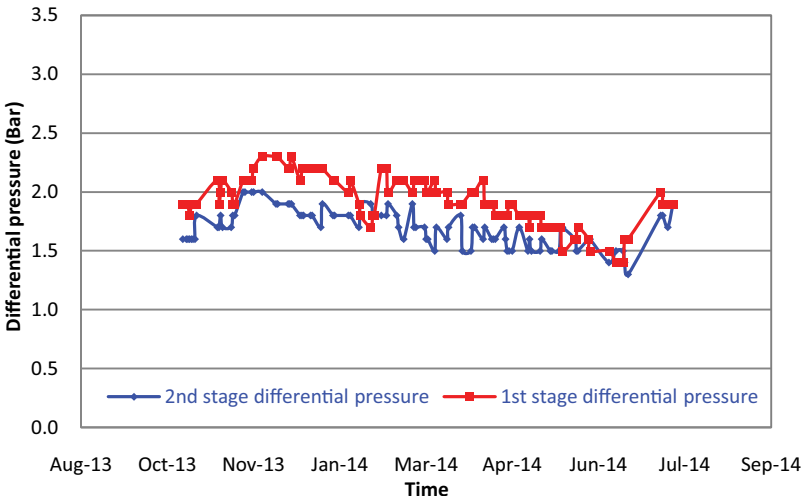

Fig. 15. Differential pressure evolution.

in the first and second stage, respectively (Fig. 13). The feed pressure ups and downs have substantially impacted the other operating measures including the permeate flow, pressure drop, and permeate conductivity (Figs. 14–16). The permeate flow rate increased by about 14.3% in the first stage and decreased by about 60% in the second stage (Fig. 10). The first stage production flow rate increase is explicated by the automatic regulation PID, connected to the frequency regulator of the high-pressure pump. This control insure the production controlling set point flow in relation to the flow measurement. It offsets the flux decay in the second stage by boosting the first stage flux [30,38].

The differential pressure has risen to a certain extent in the first stage as a consequence of the flux rise; likewise, it declined in the second stage (Fig. 9), as a result of the flux decreasing across the membranes as a consequence of the second stage membrane fouling [30,38] (Fig. 10).

The first stage permeates conductivity was steady (Fig. 12); moreover, it raised in the second stage as a consequence of the salt passage increase, caused by the possible precipitation of the salts comprised in the feed water on the membrane area, particularly, the salts NaCl, $CaCO_3$, and $CaSO_4$ [30,38].

To control the fouling and restitute the initial performance of RO membranes [53], the membrane manufacturer recommended to perform a standard chemical cleaning, utilizing basic (1% 4Na-EDTA + 0.1% NaOH) and acidic (0.2% HCl) chemical solutions [30,38,54,55].

In preference, membrane cleaning is carried out when the permeate flow drops by 10% and it will be necessarily finished when the performance is enhanced by 15% [56,57]. Allowing the RO unit in operation for a long time without chemical cleaning can generate membrane irreversible fouling [38,57].

Basic chemicals including sodium hydroxide (NaOH) clean off organic fouling and biofouling by hydrolysis and solubilization; instead, acid agents including hydrochloric acid (HCl) disperse inorganic fouling, break up the composition of the bacterial cell wall and promote precipitation of proteins [24,30,38,53,58]. Concerning RO membranes,

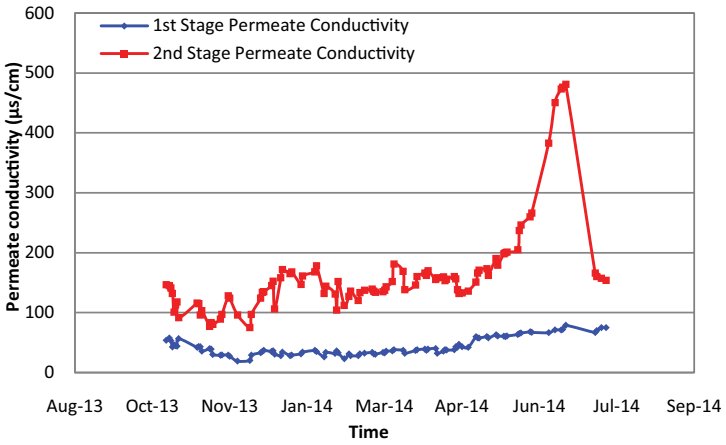

Fig. 16. Permeate conductivity evolution.

cleaning procedures involve various steps of high flow recirculation and soaking [30], enduring all over between 6.5 and 24 h in period at a usual temperature of 35°C [30,38,53].

The acidic solution was carried out in order to disperse the salts precipitated on the membrane surface, especially, NaCl, $CaCO_3$, and $CaSO_4$ contained in the surface water [30,38]. The basic solution was applied to eliminate organic fouling in particular biomass, which might be generated by eventual bacterial development or by the organic matter included in the raw surface water [30,38]. The first operation of chemical cleaning has been much successful. Indeed, the start-up flow rate of the first stage and second stage were recovered [38].

5. Rosa projection vs. RO actual performances

Tables 4 and 5 show the operating results vs. the expected design values after nearly 1 y of operation. The results presented correspond to the average values obtained during the monitoring period.

The results in Table 4 indicate that the TDS and the other ions concentration were below the expected design values due to the TDS decrease during the winter owing to the rainfall dilution process [30]. The comparison of the ROSA expected values with the experimental results prove that the RO membranes exhibit high and stable performances [30].

Throughout the whole period of operation the feed pressure, the feed flow, the permeate flow, the rejection flow, and the recovery rate of the train were close to the expected design values [30].

Table 4
Comparison of the permeate ion analysis with ROSA projection results

Parameters	RO TRAIN			
	First stage		Second stage	
	ROSA	Actual	ROSA	Actual
K (mg/L)	1.44	0.15	2.58	0.4
Na (mg/L)	29.19	10.8	75.27	39.7
Mg (mg/L)	1.13	0.5	2.95	0.52
Ca (mg/L)	4.77	1.15	12.5	1.2
HCO_3 (mg/L)	9.99	3.2	25.9	7.4
NO_3 (mg/L)	4.24	0.8	6.79	2.4
Cl (mg/L)	48.79	14.5	127.23	49
SO_4 (mg/L)	1.55	1.2	4.13	1.68
TDS (mg/L)	101.58	37	258.52	139

Table 5
Comparison of operating results with ROSA projection after 1 y of operation

Parameters	RO TRAIN			
	First stage		Second stage	
	ROSA	Actual	ROSA	Actual
Feed flow (m^3/h)	506	507.96	208.76	209.16
Feed pressure (bar)	10.54	10.7	8.99	8.6
Permeate flow (m^3/h)	297.24	298.8	112.89	111.6
Rejection flow (m^3/h)	208.76	209.16	95.87	97.56
Recovery rate (%)	58.7	58.8	54.1	53.4

6. Conclusion

This paper represents the pretreatment process optimization and the RO performance assessment of the Khenifra demineralization plant after approximately 1 y of exploitation. A number of conclusions can be drawn:

- The sludge recirculation at the flocculation level reduced coagulant consumption of about 25% and significantly reduced the turbidity.
- The sludge recirculation minimized the rapid clogging of the sand filters and therefore reduced the number of washing.
- The lowest residual Al value was obtained at pH 6.5 based on the actual quality of the surface water.
- The microfiltration using 5 µm cartridges improved significantly the SDI values.

- The antiscalant contributed to the organic matter augmentation inlet of the RO membranes.
- ROSA software predicted the performance of FILMTEC™ XLE440 close to the real industrial data.

RO membrane at large industrial scale needs to take into account the industrial feedback in the design phase and rigorous technical care at the start-up and a keen technical follow up to reach a steady stabilized performance.

References

[1] G. Adeniji-Oloukoi, B. Urmilla, M. Vadi, Households' coping strategies for climate variability related water shortages in Oke-Ogun region, Nigeria, Environ. Dev., 5 (2013) 23–38.

[2] A.-P. Avrin, G. He, D.M. Kammen, Assessing the impacts of nuclear desalination and geoengineering to address China's water shortages, Desalination, 360 (2015) 1–7.

[3] L. Garcia-Cuerva, E.Z. Berglund, A.R. Binder, Public perceptions of water shortages, conservation behaviors, and support for water reuse in the U.S., Resour. Conserv. Recycl., 113 (2016) 106–115.

[4] M.R. Hibbs, L.K. McGrath, S. Kang, A. Adout, S.J. Altman, M. Elimelech, C.J. Cornelius, Designing a biocidal reverse osmosis membrane coating: synthesis and biofouling properties, Desalination, 380 (2016) 52–59.

[5] A.R. Bartman, E. Lyster, R. Rallo, P.D. Christofides, Y. Cohen, Mineral scale monitoring for reverse osmosis desalination via real-time membrane surface image analysis, Desalination, 273 (2011) 64–71.

[6] H. Gu, A.R. Bartman, M. Uchymiak, P.D. Christofides, Y. Cohen, Self-adaptive feed flow reversal operation of reverse osmosis desalination, Desalination, 308 (2013) 63–72.

[7] J.M. Ochando-Pulido, M.D. Víctor-Ortega, A. Martínez-Ferez, Membrane fouling insight during reverse osmosis purification of pretreated olive mill wastewater, Sep. Purif. Technol., 168 (2016) 177–187.

[8] F. Tang, H.-Y. Hu, L.-J. Sun, Y.-X. Sun, N. Shi, J.C. Crittenden, Fouling characteristics of reverse osmosis membranes at different positions of a full-scale plant for municipal wastewater reclamation, Water Res., 90 (2016) 329–336.

[9] L. Lin, C. Feng, R. Lopez, O. Coronell, Identifying facile and accurate methods to measure the thickness of the active layers of thin-film composite membranes – a comparison of seven characterization techniques, J. Membr. Sci., 498 (2016) 167–179.

[10] A. Ruiz-García, E. Dimitriou, I. Nuez, Retrofitting assessment of a full-scale brackish water reverse osmosis desalination plant with a feed capacity of 600 m^3/d, Desal. Water Treat., 144 (2019) 72–78.

[11] A.A. Alsarayreh, M.A. Al-Obaidi, A.M. Al-Hroub, R. Patel, I.M. Mujtaba, Evaluation and minimisation of energy consumption in a medium-scale reverse osmosis brackish water desalination plant, J. Cleaner Prod., 248 (2020), doi: 10.1016/j.jclepro.2019.119220.

[12] A. Ruiz-García, I. de la Nuez Pestana, Feed spacer geometries and permeability coefficients. Effect on the performance in BWRO spriral-wound membrane modules, Water, 11 (2019), doi: 10.3390/w11010152.

[13] M. Li, Optimal plant operation of brackish water reverse osmosis (BWRO) desalination, Desalination, 293 (2012) 61–68.

[14] A. Ruiz-García, E. Ruiz-Saavedra, 80,000 h operational experience and performance analysis of a brackish water reverse osmosis desalination plant. Assessment of membrane replacement cost, Desalination, 375 (2015) 81–88.

[15] W.L. Ang, D. Nordin, A.W. Mohammad, A. Benamor, N. Hilal, Effect of membrane performance including fouling on cost optimization in brackish water desalination process, Chem. Eng. Res. Des., 117 (2017) 401–413.

[16] A. Ruiz-García, N. Melián-Martel, V. Mena, Fouling characterization of RO membranes after 11 years of operation in a brackish water desalination plant, Desalination, 430 (2018) 180–185.

[17] S. Farhat, M. Bali, F. Kamel, Membrane autopsy to provide solutions to operational problems of Jerba brackish water desalination plant, Desalination, 445 (2018) 225–235.

[18] S. Mondal, Methods of dye removal from dye house effluent—an overview, Environ. Eng. Sci., 25 (2008) 383–396.

[19] R.A. Al-Juboori, T. Yusaf, Biofouling in RO system: mechanisms, monitoring and controlling, Desalination, 302 (2012) 1–23.

[20] L. Henthorne, B. Boysen, State-of-the-art of reverse osmosis desalination pretreatment, Desalination, 356 (2015) 129–139.

[21] T. Nguyen, F. Roddick, L. Fan, Biofouling of water treatment membranes: a review of the underlying causes, monitoring techniques and control measures, Membranes, 2 (2012) 804–840.

[22] S. Robinson, S.Z. Abdullah, P. Bérubé, P. Le-Clech, Ageing of membranes for water treatment: linking changes to performance, J. Membr. Sci., 503 (2016) 177–187.

[23] A. Ruiz-García, N. Melián-Martel, I. Nuez, Short review on predicting fouling in RO desalination, Membranes, 7 (2017), doi: 10.3390/membranes7040062.

[24] S. Jiang, Y. Li, B.P. Ladewig, A review of reverse osmosis membrane fouling and control strategies, Sci. Total Environ., 595 (2017) 567–583.

[25] V. Campos, A.R.A.C. Fernandes, T.A.M. Medeiros, E.L. Andrade, Physicochemical characterization and evaluation of PGA bioflocculant in coagulation–flocculation and sedimentation processes, J. Environ. Chem. Eng., 4 (2016) 3753–3760.

[26] L. Rizzo, G. Lofrano, M. Grassi, V. Belgiorno, Pre-treatment of olive mill wastewater by chitosan coagulation and advanced oxidation processes, Sep. Purif. Technol., 63 (2008) 648–653.

[27] H. Xu, F. Xiao, D. Wang, Effects of Al_2O_3 and TiO_2 on the coagulation process by $Al_2(SO_4)_3$ (AS) and poly-aluminum chloride (PACl) in kaolin suspension, Sep. Purif. Technol., 124 (2014) 9–17.

[28] X. Wu, X. Ge, D. Wang, H. Tang, Distinct coagulation mechanism and model between alum and high Al13-PACl, Colloids Surf., A, 305 (2007) 89–96.

[29] R. Jiao, H. Xu, W. Xu, X. Yang, D. Wang, Influence of coagulation mechanisms on the residual aluminum – the roles of coagulant species and MW of organic matter, J. Hazard. Mater., 290 (2015) 16–25.

[30] H. Boulahfa, S. Belhamidi, F. Elhannouni, M. Taky, A. El Fadil, A. Elmidaoui, Demineralization of brackish surface water by reverse osmosis: the first experience in Morocco, J. Environ. Chem. Eng., 7 (2019), doi: 10.1016/j.jece.2019.102937.

[31] T. Harif, M. Khai, A. Adin, Electrocoagulation versus chemical coagulation: coagulation/flocculation mechanisms and resulting floc characteristics, Water Res., 46 (2012) 3177–3188.

[32] S.Y. Lee, G.A. Gagnon, Comparing the growth and structure of flocs from electrocoagulation and chemical coagulation, J. Water Process Eng., 10 (2016) 20–29.

[33] J. Wang, D. Qu, M. Tie, H. Ren, X. Peng, Z. Luan, Effect of coagulation pretreatment on membrane distillation process for desalination of recirculating cooling water, Sep. Purif. Technol., 64 (2008) 108–115.

[34] T. Okuda, A.U. Baes, W. Nishijima, M. Okada, Improvement of extraction method of coagulation active components from *Moringa oleifera* seed, Water Res., 33 (1999) 3373–3378.

[35] Z. Yang, B. Gao, Q. Yue, Coagulation performance and residual aluminum speciation of $Al_2(SO_4)_3$ and polyaluminum chloride (PAC) in Yellow River water treatment, Chem. Eng. J., 165 (2010) 122–132.

[36] H. Xu, D. Zhang, Z. Xu, Y. Liu, R. Jiao, D. Wang, Study on the effects of organic matter characteristics on the residual aluminum and flocs in coagulation processes, J. Environ. Sci., 63 (2018), 307–317.

[37] Z.L. Yang, B.Y. Gao, Q.Y. Yue, Y. Wang, Effect of pH on the coagulation performance of Al-based coagulants and residual aluminum speciation during the treatment of humic acid–kaolin synthetic water, J. Hazard. Mater., 178 (2010) 596–603.

[38] H. Boulahfa, S. Belhamidi, F. Elhannouni, M. Taky, A. El Fadil, A. Elmidaoui, Impact of the raw water seasonal variations on

the reverse osmosis performance: Khenifra Plant, Morocco, J. Water Environ. Technol., 17 (2019) 359–374.
[39] H. Zidouri, Desalination of Morocco and presentation of design and operation of the Laayoune seawater reverse osmosis plant, Desalination, 131 (2000) 137–145.
[40] N.b. Ibrahim, H.A. Aziz, Trends on natural organic matter in drinking water sources and its treatment, Int. J. Sci. Res. Environ. Sci., 2 (2014) 94–106.
[41] M. Sillanpää, M.C. Ncibi, A. Matilainen, M. Vepsäläinen, Removal of natural organic matter in drinking water treatment by coagulation: a comprehensive review, Chemosphere, 190 (2018), 54–71.
[42] J. Xie, D. Wang, J. van Leeuwen, Y. Zhao, L. Xing, C.W.K. Chow, pH modeling for maximum dissolved organic matter removal by enhanced coagulation, J. Environ. Sci., 24 (2012) 276–283.
[43] F. Xiao, M.F. Simcik, J.S. Gulliver, Mechanisms for removal of perfluorooctane sulfonate (PFOS) and perfluorooctanoate (PFOA) from drinking water by conventional and enhanced coagulation, Water Res., 47 (2013) 49–56.
[44] F.K. Katrivesis, A.D. Karela, V.G. Papadakis, C.A. Paraskeva, Revisiting of coagulation–flocculation processes in the production of potable water, J. Water Process Eng., 27 (2019) 193–204.
[45] J. Qin, M. Oo, K. Kekre, F. Knops, P. Miller, Impact of coagulation pH on enhanced removal of natural organic matter in treatment of reservoir water, Sep. Purif. Technol., 49 (2006) 295–298.
[46] J. Gregory, J. Duan, Hydrolyzing metal salts as coagulants, Pure Appl. Chem., 73 (2001) 2017–2026.
[47] J.S. Vrouwenvelder, S.A. Manolarakis, H.R. Veenendaal, D. van der Kooij, Biofouling potential of chemicals used for scale control in RO and NF membranes, Desalination, 132 (2000) 1–10.
[48] J.S. Vrouwenvelder, F. Beyer, K. Dahmani, N. Hasan, G. Galjaard, J.C. Kruithof, M.C.M. Van Loosdrecht, Phosphate limitation to control biofouling, Water Res., 44 (2010) 3454–3466.
[49] A. Sweity, Y. Oren, Z. Ronen, M. Herzberg, The influence of antiscalants on biofouling of RO membranes in seawater desalination, Water Res., 47 (2013) 3389–3398.
[50] A. Alhadidi, B. Blankert, A.J.B. Kemperman, J.C. Schippers, M. Wessling, W.G.J. van der Meer, Effect of testing conditions and filtration mechanisms on SDI, J. Membr. Sci., 381 (2011) 142–151.
[51] C. Riverol, M.V. Pilipovik, Prediction of the behaviour of the silt density index (SDI) in the Caribbean Seawater and its impact on RO desalination plants, Desalination, 268 (2011) 262–265.
[52] M. Habib, U. Habib, A.R. Memon, U. Amin, Z. Karim, A.U. Khan, S. Naveed, S. Ali, Predicting colloidal fouling of tap water by silt density index (SDI): pore blocking in a membrane process, J. Environ. Chem. Eng., 1 (2013) 33–37.
[53] F. Beyer, J. Laurinonyte, A. Zwijnenburg, A.J.M. Stams, C.M. Plugge, Membrane fouling and chemical cleaning in three full-scale reverse osmosis plants producing demineralized water, J. Eng., 2017 (2017) 1–14.
[54] D.N. Nada, Large SWRO project for drinking water in Shuqaiq, Int. Desal. Assoc., (2011).
[55] L. Zheng, D. Yu, G. Wang, Z. Yue, C. Zhang, Y. Wang, J. Zhang, J. Wang, G. Liang, Y. Wei, Characteristics and formation mechanism of membrane fouling in a full-scale RO wastewater reclamation process: membrane autopsy and fouling characterization, J. Membr. Sci., 563 (2018) 843–856.
[56] Dow Water and Process Solutions FILMTEC™ Reverse Osmosis Membranes Technical Manual. Available at: http://msdssearch.dow.com/PublishedLiteratureDOWCOM/dh_095b/0901b8038095b91d.pdf?filepath=liquidseps/pdfs/noreg/609–00071.pdf (accessed October 17, 2018).
[57] A. Ruiz-García, I. Nuez, Long-term performance decline in a brackish water reverse osmosis desalination plant. Predictive model for the water permeability coefficient, Desalination, 397 (2016) 101–107.
[58] Hydranautics, Technical Service Bulletin Foulants and Cleaning Procedures for Composite Polyamide RO Membrane Elements (ESPA, ESNA, CPA, LFC, NANO and SWC), 2014. Available at: http://membranes.com/docs/tsb/TSB107.pdf (accessed January 1, 2019).